

VLLaVO: Mitigating Visual Gap through LLMs

Shuhao Chen^{1*}, Yulong Zhang^{2*}, Weisen Jiang^{1,3}, Jiangang Lu², and
Yu Zhang^{1**}

¹ Southern University of Science and Technology

² Zhejiang University

³ Hong Kong University of Science and Technology

Project Page: <https://ll-a-vo.github.io/>

Abstract. Recent advances achieved by deep learning models rely on the independent and identically distributed assumption, hindering their applications in real-world scenarios with domain shifts. To tackle this issue, cross-domain learning aims at extracting domain-invariant knowledge to reduce the domain shift between training and testing data. However, in visual cross-domain learning, traditional methods concentrate solely on the image modality, disregarding the potential benefits of incorporating the text modality. In this work, we propose VLLaVO, combining Vision language models and Large Language models as Visual cross-domain learners. VLLaVO uses vision-language models to convert images into detailed textual descriptions. A large language model is then finetuned on textual descriptions of the source/target domain generated by a designed instruction template. Extensive experimental results under domain generalization and unsupervised domain adaptation settings demonstrate the effectiveness of the proposed method.

Keywords: Domain Generalization · Unsupervised Domain Adaptation
· Large Language Models

1 Introduction

Deep models have achieved promising performance in various applications of computer vision when testing images are sampled from the same distribution of training data [51, 52, 67, 74]. However, in real-world applications, domain shifts [99] remain a significant challenge due to the distribution discrepancy between training and testing domains. For instance, an autonomous driving car should be able to handle adverse weather which does not appear during the training stage [5–7], posing a substantial hurdle for model generalization. To alleviate the domain shift, cross-domain learning [18, 81, 82] aims at extracting domain-invariant knowledge between source and target domains.

Typical cross-domain learning scenarios include domain generalization (DG) [19, 22, 49] and unsupervised domain adaptation (UDA) [1, 10, 16, 18]. Specifically, DG

* Equal contribution.

** Corresponding author.

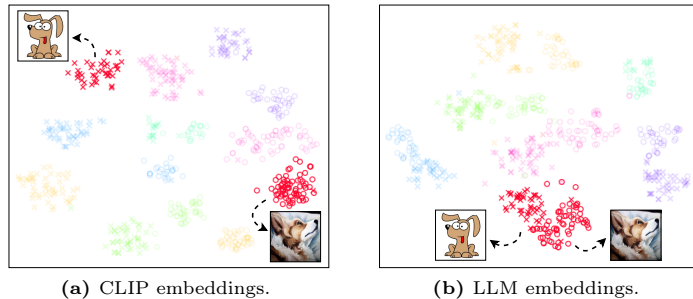


Fig. 1: t-SNE visualizations of samples from the Art Painting domain (marked by “o”) and the Cartoon domain (marked by “x”) on the *PACS* dataset. Samples of the same category are depicted in the same color. Implementation details are provided in Section 4.4.

trains a model from multiple source domains and evaluates it on an unseen target domain, while UDA assumes some unlabeled data from the target domain is available for training. Various DG [21, 103, 105] and UDA [16, 18, 104] methods have been proposed to alleviate the domain shift by learning domain-invariant features in the image modality. For example, under the DG setting, MIRO [21] proposes to learn features that are similar to the oracle representation. For the UDA setting, BCAT [107] leverages a bidirectional cross-attention mechanism to extract implicit source and target mixup feature representations. However, the above methods only utilize the image modality for cross-domain learning.

Instead of just using the image modality, recent efforts on large-scale vision-language models (VLMs) [23, 56, 100] have shown significant improvements in image classification by learning from massive paired image-text samples. For example, CLIP [23], which consists of an image encoder and a text encoder, is trained on 400 million image-text pairs by contrastive learning [101]. However, as shown in Figure 1a, learning domain-invariant features based on CLIP is challenging due to the large domain shift, leading to sub-optimal cross-domain performance. On the other hand, large language models (LLMs) [27, 72] have impressive zero-shot capability for text-based tasks. Nevertheless, it is essential to acknowledge that the success of LLMs does not readily extend to pure vision and vision-language tasks, primarily due to the inherent disparities in modalities and task structures. To the best of our knowledge, there is no work that integrates LLMs with visual cross-domain learning.

In this paper, we propose VLLaVO, combining Vision language models and Large Language models as Visual cross-dOmain learners, to integrate the powerful LLMs into visual cross-domain learning. Firstly, we use various VLMs (including CLIP [23] and BLIP [30]) to convert images into detailed textual descriptions (*i.e.*, tags, attributes, and captions). As shown in Example 2 placed in the experimental section, these descriptions contain crucial image content information. As a byproduct, based on these descriptions, we release a series of datasets in text modality for text classification tasks and the details are given in Appendix B. Next, we design an instruction template for querying the LLM to

obtain images’ categories based on their descriptions. However, the domain shift of generated textual descriptions still exists across domains. A straightforward method *rank classification* [27] employs the output probability of LLM for each category to perform classification. Empirical results indicate that this simple method performs poorly in challenging cross-domain tasks due to distractions from irrelevant contexts [70, 95, 96] and the issue of hallucinations [53, 69, 97]. Especially in cross-domain learning scenarios, there are many domain-specific but class-irrelevant contexts [99]. To deal with these challenges, we finetune the LLM using training data comprised of question-answer pairs, where the questions are created by the proposed template and the answers correspond to the class tokens of corresponding images. To better adapt VLLaVO in the UDA scenario, we utilize the available target domain data with its pseudo-labels to further finetune the LLM. Experiments conducted on benchmark datasets under the DG and UDA settings have demonstrated that the proposed VLLaVO method achieves state-of-the-art performance. Moreover, compared with existing VLM-based methods, VLLaVO performs better, showing the benefits of integrating LLM into cross-domain learning. Additional support can be gained from the smaller domain shift of LLM than that of VLM (*i.e.*, CLIP), as shown in Figure 1.

Our contributions are summarized as follows.

- We are the first to utilize LLMs for visual cross-domain learning. The proposed VLLaVO uses VLMs for bridging image and text modalities and designs a question instruction template for the LLM to predict the category of an image based on its description.
- The introduced VLLaVO alleviates domain shifts through the inherent generalization capability of LLM. Finetuning LLM on the designed question instruction template enhances its instruction-following ability, reducing the distractions of irrelevant contexts.
- Extensive experiments on diverse DG and UDA tasks demonstrate that VLLaVO consistently achieves state-of-the-art performance, surpassing existing VLM-based methods.
- To facilitate further research, we release a series of datasets in the text modality, including *PACS*, *OfficeHome*, and *DomainNet*.

2 Related Work

The goal of cross-domain learning [81, 82] is to learn a model from the source domain(s) with the possible help of the target domain to learn domain-invariant features and apply them to the target domain. Domain generalization and unsupervised domain adaptation are two typical scenarios in cross-domain learning. **Domain Generalization (DG)**. DG [21, 22, 49, 83] aims to improve the generalization capabilities of the models in new domains that are unseen during the training phase. DG is widely used in real-world applications [83, 84] and various methods have been proposed. For example, SWAD [22] and SAGM [49]

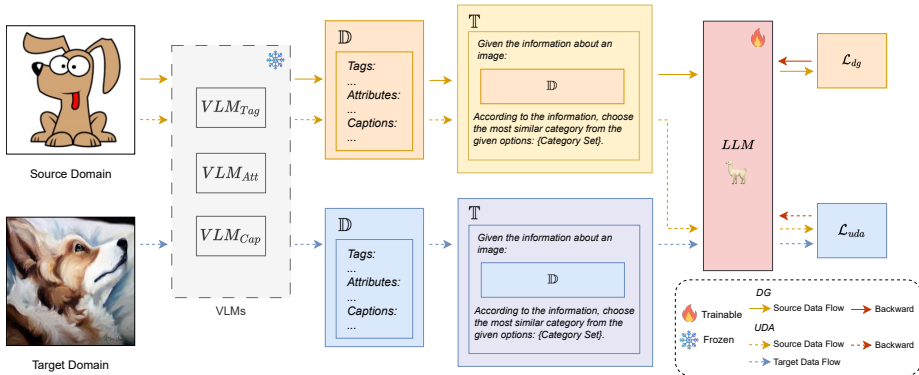


Fig. 2: An illustration of the proposed VLLaVO framework for both UDA and DG. For DG, the source images are converted into the text modality through the VLMs. Then, the extracted descriptions are used to finetune an LLM. For UDA, we use the target domain samples with pseudo-labels and the source domain samples with ground truth labels to finetune the LLM.

find flatter minima to improve the generalization capabilities. Instead of learning domain-invariant features, MIRO [21] is proposed to learn features that are similar to the oracle representation.

Unsupervised Domain Adaptation (UDA). Besides a source domain with labeled data, in the UDA scenario [16, 17, 92], unlabeled data in the target domain are available during the training phase. CDTrans [18] proposes a weight-sharing triple-branch transformer framework to enhance feature alignment and improve robustness to noisy pseudo-labels. From a perspective of game theory, PMTrans [92] builds up an intermediate domain with an effective ViT [74]-based solution to smoothly bridge the source and target domains. Instead of explicitly aligning the source and target domains, MCC [17] introduces a general class confusion loss as a regularizer. ELS [16] adopts the domain adversarial training strategy, and mitigates the impact of label noise by encouraging the domain discriminator to output soft domain labels.

However, most existing DG and UDA methods focus solely on the image modality, leading to sub-optimal cross-domain effects as shown in our experiments. On the contrary, our VLLaVO further leverages the text modalities.

VLMs and LLMs. VLMs have shown promising performance in learning visual representations [9, 26, 55, 58]. A notable example is CLIP [23], which is trained on 400 million image-text pairs and has been applied to various downstream tasks [56, 59, 65]. Recently, some works have applied CLIP to address domain shift problems [8, 60]. For example, DPL [65] learns a lightweight prompt generator to generate a domain-specific prompt for efficiently adapting CLIP to an unseen domain. CLIPood [19] further leverages the semantic relationships between classes in the text modality and proposes a novel model optimization strategy to improve the generalization performance. PADCLIP [10] proposes a catastrophic forgetting metric to adjust the learning rate and alleviate the catas-

trophic forgetting issue of CLIP. However, finetuning CLIP directly leads to a sacrifice in cross-domain generalization capability [10, 19].

On the other hand, LLMs show impressive generalization capability in various natural language processing tasks, *e.g.*, topic classification [2, 27], mathematical reasoning [3, 4, 78, 79], and question answering [27, 28, 77]. Moreover, instruction-tuning methods [28, 85, 87] further improve the zero-shot and few-shot performance of LLM. Despite these advancements, LLMs cannot be directly applied to pure vision tasks and vision-language tasks due to the inherent disparities in modalities and task structure. To address this issue, some works have utilized VLMs as a bridge between the image and text modalities. For example, Menon et al. [9] leverage an LLM (*i.e.*, GPT-3 [27]) to obtain descriptions for each category and employ CLIP to make predictions based on both the images and the extracted textual descriptions. LENS [25] designs a set of highly descriptive visual modules based on VLMs, enabling LLMs to tackle visual tasks. Different from those works that assume that all the data are in the same domain, the proposed VLLaVO focuses on visual cross-domain learning.

3 Methodology

3.1 Overview of The Entire Framework

Suppose there is a set of S source domains $\{\mathcal{D}_i\}_{i=1}^S$, where $\mathcal{D}_i = \{(\mathbf{x}_j^i, y_j^i)\}_{j=1}^{n_i}$ and n_i denotes the number of samples in \mathcal{D}_i . Let $\mathcal{D} = \cup_{i=1}^S \mathcal{D}_i$ denote the entire source domain training data. In cross-domain learning, we aim to learn a model from source domains and then generalize the model to a target domain \mathcal{T} whose data distribution differs from that of the source domains. In DG, target domain data are unavailable during the training process, while in the training process of UDA, the unlabeled target domain data are available. In UDA, S equals to 1.

To begin with, VLLaVO generates textual descriptions of images using pre-trained VLMs. These obtained textual descriptions still exhibit domain shifts. Thus, we finetune an LLM with the designed question instruction template that combines these descriptions and their category labels. Finetuning enables the LLM to follow the question instruction template and focus on the domain-invariant information related to the classification. The overall framework of VLLaVO is shown in Figure 2 and the entire algorithm is shown in Algorithm 1 of Appendix C. In the following sections, we will detail each step individually.

3.2 Generating Textual Descriptions for Images

For an image \mathbf{x} , we use VLMs to convert it into textual descriptions. Previous works [9, 61] have demonstrated that textual descriptions can provide information for classification. Following [25], we use pretrained VLMs to extract textual descriptions from three aspects: (i) Tags; (ii) Attributes; and (iii) Captions.

To extract tags, a comprehensive tag vocabulary is constructed by integrating diverse sources, including multiple datasets such as [37–48]. Specifically, the tags

are wrapped by a standardized template “A photo of {tag}” and then fed to the text encoder of the CLIP model to obtain the embeddings. For each image \mathbf{x} , we compute the cosine similarity between its embedding extracted by the image encoder of the CLIP model and tags’ embeddings. The Top- K similar tags are then used in the textual description.

However, tags are usually too brief to contain detailed descriptions of images. To deal with this issue, we use GPT-3 [27] to enrich the tags with attribute information. Specifically, for each tag, we prompt GPT-3 with the input “What are useful features for distinguishing a {tag} in a photo?” to generate the crucial attributes of visual characteristics for each tag. Similarly, all attributes are fed into the text encoder of the CLIP model to obtain the embeddings. For each image \mathbf{x} , we first calculate the cosine similarity between the embedding of \mathbf{x} , extracted by the image encoder of the CLIP model, and the embeddings of the attributes. Then the Top- M attributes with the highest similarity scores are used in the textual description.

As tags and attributes are concept-level descriptions of images, they lack specific content of images. To this end, we further enrich the textual information by extracting captions of images. We use an image captioning model (*e.g.*, BLIP [30]) to generate Top- N captions for each image by stochastic sampling [29].

Based on the extracted tags, attributes, and captions as described above, we can obtain the textual descriptions as

$$\begin{aligned} \mathbb{D}(\mathbf{x}) = & \text{“Tags: \{Top-}K \text{ tags\}} \\ & \text{Attributes: \{Top-}M \text{ attributes\}} \\ & \text{Captions: \{Top-}N \text{ captions\}} \text{”} . \end{aligned}$$

For illustration, Example 2 shows an example image and its corresponding extracted description.

3.3 Question Instruction

After extracting textual descriptions from images, we can use LLM for classification. Specifically, we design a question instruction template for querying the LLM to its category. The template $\mathbb{T}(\mathbf{x})$ is shown in Example 1, where $\{\mathbb{D}(\mathbf{x})\}$ denotes the placeholder of the textual description of \mathbf{x} and $\{\text{Category Set}\}$ is the placeholder of the candidate categories. An example of the category set is shown in Appendix A.1.

Example 1: Template $\mathbb{T}(\mathbf{x})$.

Give the information about an image: $\{\mathbb{D}(\mathbf{x})\}$.
 According to the information, choose the most similar category from the given options: $\{\text{Category Set}\}$.
 ### Answer:

3.4 Finetuning

The question instruction template with textual descriptions effectively translates cross-domain image classification tasks into text classification tasks. Zero-Shot LLM (ZS-LLM) [28] feeds $\mathbb{T}(\mathbf{x})$ into LLM and computes the sum of per-token log-likelihood for each category to apply *rank classification* [27]. The category with the highest log-likelihood is chosen as the predicted category. However, as shown in Figure 3a, ZS-LLM performs poor in cross-domain tasks because (1) As shown in Table 8, the distribution of textual description is still different across domains. LLM are susceptible to the influence of irrelevant context (*e.g.*, domain-specific words) within the descriptions, which can negatively impact their classification accuracy [70]. (2) The output of LLM is correlated to but still misaligned with the ground-truth category [98]. See Appendix E.2 for further discussion.

To address the above issues and further exploit the capabilities of LLM in classifying samples based on textual descriptions, we formulate the classification problem as a question-answer problem $(\mathbb{T}(\mathbf{x}), y)$, where y , the class label of \mathbf{x} , is represented by a sequence of class tokens and denotes the true answer to the question $\mathbb{T}(\mathbf{x})$.

Finetuning for DG Tasks Under the setting of DG, inspired by [22, 102], we assume that there exists a global labeling function that generates labels for multiple domains. Thus we combine the training datasets of all the source domains into a training dataset \mathcal{D} . Then, instruction tuning is conducted on $\{(\mathbb{T}(\mathbf{x}), y) : (\mathbf{x}, y) \in \mathcal{D}\}$ with the next-token prediction objective. As LLMs have billions of parameters (*e.g.*, LLaMA2 series have 7B, 13B, and 70B parameters), fully finetuning the LLM is computationally expensive. Therefore, we adopt the widely used parameter-efficient finetuning strategy (*i.e.*, LoRA [31]). Let θ denote parameters in the LoRA modules. Formally, the training objective of DG is to minimize the training loss as

$$\mathcal{L}_{dg}(\theta) = - \sum_{(\mathbf{x}, y) \in \mathcal{D}} \log p_{\theta}(y | \mathbb{T}(\mathbf{x})). \quad (1)$$

Finetuning for UDA Tasks To make VLLaVO more suitable for UDA tasks, we propose the utilization of VLLaVO in conjunction with pseudo-labeling techniques. Pseudo-labeling strategies [34, 35] have enjoyed success in UDA by leveraging the unlabeled target domain data [10, 36]. Under the UDA setting, VLLaVO combines target domain samples with pseudo-labels and source domain samples with ground truth labels to finetune the LLM. Similar to Eq. (1), the pseudo-labeling-based finetuning objective of UDA is to minimize the training loss as

$$\mathcal{L}_{uda}(\theta) = - \sum_{(\mathbf{x}, y) \in \mathcal{D}} \log p_{\theta}(y | \mathbb{T}(\mathbf{x})) - \sum_{\mathbf{x} \in \mathcal{T}} \log p_{\theta}(\hat{y} | \mathbb{T}(\mathbf{x})), \quad (2)$$

where \hat{y} denotes the pseudo-label for each target domain sample. Specifically, the LLM is first finetuned using the source domain training data \mathcal{D} with a loss

Table 1: Testing accuracies (%) of DG tasks on the *PACS*, *OfficeHome*, and *DomainNet* datasets. n/a denotes not applicable. The best is in **bold**.

	<i>PACS</i>					<i>OfficeHome</i>					<i>DomainNet</i>						
	A	C	P	S	Avg	A	C	P	R	Avg	C	I	P	Q	R	S	Avg
ERM-ResNet [11]	84.7	80.8	97.2	79.3	85.5	61.3	52.4	75.8	76.6	66.5	58.1	18.8	46.7	12.2	59.6	49.8	40.9
SWAD [22]	89.3	83.4	97.3	82.5	88.1	66.1	57.7	78.4	80.2	70.6	66.0	22.4	53.5	16.1	65.8	55.5	46.5
SAGM [49]	87.4	80.2	98.0	80.8	86.6	65.4	57.0	78.0	80.0	70.1	64.9	21.1	51.5	14.8	64.1	53.6	45.0
MIRO [21]	96.3	97.3	99.7	93.9	96.8	82.4	72.2	89.1	89.3	83.3	78.9	46.3	68.9	19.3	80.8	69.7	60.7
ZS-CLIP [23]	96.4	98.9	99.9	87.7	95.7	80.7	64.6	86.3	88.0	79.9	70.7	49.1	66.4	14.8	82.7	63.1	57.8
ERM-CLIP [11]	95.8	97.2	99.6	88.4	95.3	80.0	67.6	85.8	87.6	80.3	75.1	44.7	68.1	18.4	75.7	66.2	58.0
DPL [65]	-	-	-	-	97.3	-	-	-	-	84.2	-	-	-	-	-	-	56.7
CLIPood [19]	98.9	99.6	100.0	91.2	97.4	88.0	74.0	92.8	93.2	87.0	77.6	54.7	72.5	20.7	85.7	69.9	63.5
ZS-LLM [28]	87.7	94.1	97.4	93.8	93.3	59.0	53.0	70.0	67.0	62.2	n/a	n/a	n/a	n/a	n/a	n/a	n/a
VLLaVO	99.5	99.7	100.0	94.8	98.5	90.0	86.7	97.4	95.1	92.3	83.7	56.7	75.1	21.3	87.8	74.4	66.5

function identical to Eq. (1). Subsequently, the finetuned LLM is employed to generate pseudo-labels for target domain samples.

3.5 Inference

After finetuning LLM with the designed question instruction template, the LLM can make predictions from the category set. Thus, we use the finetuned LLM to evaluate the samples in the target domain \mathcal{T} for both DG and UDA settings. Specifically, given a testing sample \mathbf{x} , we feed the wrapped question $\mathbb{T}(\mathbf{x})$ to the finetuned LLM to generate its answer as the prediction.

4 Experiments

In this section, we empirically evaluate the proposed VLLaVO method on both DG and UDA tasks. Section 4.1 discusses the experiments on DG tasks, and Section 4.2 discusses the experiments on UDA tasks. Additionally, to delve deeper into the capabilities of VLLaVO, we perform an ablation study in Section 4.3 and provide a detailed analysis in Section 4.4.

4.1 Experiments on DG Tasks

Datasets. Experiments are conducted on four DG benchmark datasets, including *PACS* [20], *OfficeHome* [36], and *DomainNet* [24]. Due to the page limit, the statistics of each dataset are offered in Appendix A.1. We follow the leave-one-out cross-evaluation protocol [71]: for each task, one domain is chosen as the target domain for testing, while the remaining domains serve as source domains for training.

Baselines. The proposed method is compared with existing DG methods including (i) ERM-ResNet [11], SWAD [22], MIRO [21], and SAGM [49] that use only the image modality. (ii) Zero-shot CLIP (ZS-CLIP) [23], ERM-CLIP, DPL [65], and CLIPood [19] that use both the image and text modalities. ZS-CLIP uses the pre-trained CLIP to calculate the similarity between the query image embedding

Table 2: Testing accuracies (%) of UDA tasks on the *OfficeHome* dataset. The best is in **bold**.

	A→C	A→P	A→R	C→A	C→P	C→R	P→A	P→C	P→R	R→A	R→C	R→P	Avg
ERM [11]	44.1	67.1	74.3	53.3	62.0	64.5	51.9	38.9	72.9	64.5	43.8	75.4	59.4
DANN [13]	52.5	62.6	73.2	56.9	67.0	68.3	58.4	54.1	78.3	70.8	60.8	80.6	65.3
AFN [12]	52.6	72.4	77.0	64.9	71.1	72.9	64.1	51.3	77.8	72.2	57.5	82.1	68.0
CDAN [14]	54.2	72.2	78.3	62.0	71.4	72.4	63.0	55.7	80.7	74.7	61.2	83.7	69.1
SDAT [15]	58.2	77.5	81.4	66.1	76.5	76.4	63.7	56.7	82.5	76.0	62.1	85.2	71.9
MCC [17]	56.8	79.8	82.7	67.8	77.0	77.8	67.0	55.4	81.8	74.0	61.4	85.4	72.2
ELS [16]	57.8	77.7	81.6	66.6	76.7	76.4	62.7	56.7	82.1	75.6	62.9	85.4	71.8
CDTrans [18]	68.8	85.0	86.9	81.5	87.1	87.3	79.6	63.3	88.2	82.0	66.0	90.6	80.5
PMTrans [91]	81.3	92.9	92.8	88.4	93.4	93.2	87.9	80.4	93.0	89.0	80.9	94.8	89.0
PADCLIP [10]	76.4	90.6	90.8	86.7	92.3	92.0	86.0	74.5	91.5	86.9	79.1	93.1	86.7
VLLaVO	85.4	96.6	94.1	90.3	97.1	94.4	87.9	85.7	94.5	90.1	85.5	97.3	91.6

and the text embedding from the category set, and then choose the highest one as the prediction. For ERM-CLIP, following [90], we add a classification head after the image encoder and finetune both components in the source domain. (iii) ZS-LLM [28] classifies images based on the textual descriptions. ZS-LLM and VLLaVO use the same VLMs (*i.e.*, CLIP-ViT-H-14 [23] and BLIP [30]) for extracting textual descriptions and LLM (*i.e.*, LLaMA-7B [72]) for classification. Note that the inference time of ZS-LLM grows with the number of categories, making it computationally infeasible for huge datasets like *DomainNet* (with 345 categories). Therefore, ZS-LLM is not applicable *DomainNet*. Implementation details are provided in Appendix A.2.

Results. Table 1 shows the classification accuracies in the target domain for the *PACS*, *OfficeHome*, and *DomainNet* datasets, respectively. As can be seen, VLLaVO consistently achieves the best accuracy for each task on all the datasets. VLLaVO outperforms CLIP-based methods (*i.e.*, ZS-CLIP, ERM-CLIP, DPL, and CLIPood), showing that using LLM could help VLMs in learning domain-invariant features to boost cross-domain performance. VLLaVO also outperforms ZS-LLM by a large margin (*i.e.*, *PACS*(+5.2%), *OfficeHome*(+30.1%)), showing that finetuning the LLM on the designed question instruction template can improve its ability in handling vision cross-domain problems. Those results demonstrate the effectiveness of the proposed VLLaVO method.

4.2 Experiments on UDA Tasks

Datasets. For UDA, experiments are conducted on two benchmark datasets: *OfficeHome* [36] and *DomainNet* [24]. The statistics of those datasets are provided in Table 10 of Appendix A.1.

Baselines. The proposed method is compared with various UDA methods using the image modality only, including ERM [11], DANN [13], AFN [12], CDAN [14], SDAT [15], MCC [17], ELS [16], CDTrans [18], and PMTrans [91]. We also compare with PADCLIP [10] that uses both the image and text modalities. Implementation details are provided in Appendix A.2.

Table 3: Testing accuracies (%) of UDA tasks on the *DomainNet* dataset.

ERM	C	I	P	Q	R	S	Avg	MCC	C	I	P	Q	R	S	Avg	CDTrans	C	I	P	Q	R	S	Avg
C	-	18.0	36.2	12.1	53.6	42.6	32.5	C	-	19.9	39.6	9.0	56.9	43.6	33.8	C	-	29.4	57.2	26.0	72.6	58.1	48.7
I	41.0	-	35.7	4.7	52.9	31.2	33.1	I	37.2	-	38.1	3.0	54.8	26.6	31.9	I	57.0	-	54.4	12.8	69.5	48.4	48.4
P	46.0	18.5	-	6.2	59.9	38.5	34.4	P	48.4	19.7	-	4.4	61.1	41.2	35.0	P	62.9	27.4	-	15.8	72.1	53.9	46.4
Q	13.6	1.2	2.1	-	6.0	10.2	6.6	Q	18.5	3.9	9.2	-	17.6	13.0	12.4	Q	44.6	8.9	29.0	-	42.6	28.5	30.7
R	51.8	21.8	50.3	7.4	-	38.0	33.9	R	55.1	22.5	54.0	4.7	-	37.8	34.8	R	66.2	31.0	61.5	16.2	-	52.9	45.6
S	54.8	15.6	38.6	14.1	49.9	-	34.6	S	60.0	18.7	47.3	10.3	57.9	-	38.8	S	69.0	29.6	59.0	27.2	72.5	-	51.5
Avg	42.0	15.0	32.6	8.9	44.5	32.1	29.2	Avg	43.8	16.9	37.6	6.3	49.6	32.4	32.4	Avg	59.9	25.3	52.2	19.6	65.9	48.4	45.2

PMTrans	C	I	P	Q	R	S	Avg	PADCLIP	C	I	P	Q	R	S	Avg	VLLaVO	C	I	P	Q	R	S	Avg
C	-	34.2	62.7	32.5	79.3	63.7	54.5	C	-	55.1	71.1	36.8	84.2	68.1	63.1	C	-	56.0	71.5	19.9	87.1	74.2	61.8
I	67.4	-	61.1	22.2	78.0	57.6	57.3	I	73.6	-	70.6	18.0	83.5	66.6	62.5	I	82.0	-	72.7	21.5	86.9	72.9	67.2
P	69.7	33.5	-	23.9	79.8	61.2	53.6	P	75.4	54.3	-	32.0	83.5	67.2	62.5	P	82.3	55.3	-	17.5	86.8	72.8	63.0
Q	54.6	17.4	38.9	-	49.5	41.0	40.3	Q	74.6	53.6	70.0	-	83.1	66.1	69.5	Q	79.2	52.5	66.3	-	84.8	70.7	70.7
R	74.1	35.3	70.0	25.4	-	61.1	53.2	R	76.4	54.9	72.7	31.7	-	67.5	60.6	R	83.7	55.7	74.2	18.8	-	73.6	61.2
S	73.8	33.0	62.6	30.9	77.5	-	55.6	S	76.3	54.9	71.7	34.9	83.6	-	64.3	S	83.1	55.3	75.4	21.4	87.1	-	64.4
Avg	67.9	30.7	59.1	27.0	72.8	56.9	62.9	Avg	75.3	54.6	71.2	30.7	83.6	67.1	63.7	Avg	82.1	55.0	72.0	19.8	84.2	72.8	64.7

Table 4: Effects of different textual information for DG tasks on the *OfficeHome* dataset. The best is in **bold**.

Tags	Attributes	Captions	A	C	P	R	Avg
✓	✗	✗	89.2	85.9	97.3	94.7	91.8
✗	✓	✗	88.9	85.9	96.9	94.4	91.5
✗	✗	✓	88.2	83.3	95.3	92.8	89.9
✓	✓	✓	90.5	85.8	97.4	95.4	92.3
Previous SOTA [19]			88.0	74.0	92.8	93.2	87.0

Results. Tables 2 and 3 show the testing accuracies of UDA tasks on the *OfficeHome* and *DomainNet* dataset, respectively. As can be seen, VLLaVO consistently achieves superior average accuracy on all datasets. Compared with baselines based on the image modality only (*i.e.*, ERM, DANN, AFN, CDAN, SDAT, MCC, ELS, CDTrans, and PMTrans), VLLaVO performs better on average, demonstrating the effectiveness of using both the image and text modalities. VLLaVO also has good performance for each task on all the datasets. Specifically, VLLaVO achieves the best performance on all 12 tasks and 23 of 30 tasks on the *OfficeHome* and *DomainNet* datasets, respectively. Moreover, VLLaVO outperforms the CLIP-based method (*i.e.*, PADCLIP), indicating that incorporating LLMs into cross-domain learners is more effective in cross-domain learning.

4.3 Ablation Study

Effects of Description Components By following the setting in Section 4.1, we conduct experiments to study the effects of tags, attributes, and captions in the descriptions extracted by VLMs on the performance. Table 4 shows the testing accuracy of DG tasks on the *OfficeHome* dataset. As can be seen, VLLaVO using only the tags, attributes or captions performs better than the existing SOTA method (*i.e.*, CLIPood) shown in Table 1. By using tags, attributes, and captions as descriptions, VLLaVO achieves the best performance, which demonstrates the effectiveness of using tags, attributes, and captions together. Due to page limit, experimental results of UDA tasks on the *OfficeHome* dataset are

Table 5: Effects of different models to generate descriptions for DG tasks on the *OfficeHome* dataset. The best is in **bold**.

	A	C	P	R	Avg
Previous SOTA [19]	88.0	74.0	92.8	93.2	87.0
VLLaVO (BLIP + GPT-3)	90.0	86.7	97.4	95.1	92.3
VLLaVO (GIT + GPT-3)	87.8	82.0	96.6	94.7	90.3
VLLaVO (BLIP + GPT-3.5)	89.7	86.6	97.3	95.1	92.2

Table 6: Effects of different LLM components for DG tasks on the *OfficeHome* dataset. The best is in **bold**.

	A	C	P	R	Avg
Previous SOTA [19]	88.0	74.0	92.8	93.2	87.0
VLLaVO (w/ Flan-T5-base)	85.0	81.7	92.8	90.4	87.5
VLLaVO (w/ LLaMA2-7B)	90.0	86.7	97.4	95.1	92.3

offered in Appendix A.3. Again, VLLaVO using all the text descriptions achieves the best performance.

To study the effect of different VLMs/LLMs for generating the descriptions, we replace the default caption model (*i.e.*, BLIP) with GIT [106] and the default vocabulary generating model (*i.e.*, GPT-3) with GPT-3.5, respectively. Table 5 shows the testing accuracy of DG tasks on the *OfficeHome* dataset. As can be seen, all variants of VLLaVO outperform the previous SOTA.

Effects of LLM To verify the effectiveness of LLMs used in VLLaVO, we replace the default LLaMA2-7B with Flan-T5-base [85], a language model with a different structure and much fewer parameters (*i.e.*, 250 million). Table 6 shows the testing accuracy of DG tasks on the *OfficeHome* dataset by using the setting in Section 4.1. As can be seen, VLLaVO (w/ Flan-T5-base) performs slightly better than the previous SOTA (*i.e.*, CLIPood), showing that it is flexible to choose the LLM for VLLaVO. Moreover, using a more powerful LLM for VLLaVO (*e.g.*, LLaMA2-7B) yields better performance. Table 12 of Appendix A.3 shows the testing accuracy of UDA tasks on the *OfficeHome* dataset. Again, both VLLaVO (w/ Flan-T5-base) and VLLaVO (w/ LLaMA2-7B) perform better than the previous SOTA.

Effects of Finetuning with Pseudo-Labels in UDA To verify the effectiveness of finetuning with pseudo-labels in UDA, we compare VLLaVO with its variant, VLLaVO (w/o PseudoLabels), on the *DomainNet* dataset. Here, VLLaVO (w/o PseudoLabels) represents VLLaVO without the pseudo-labeling-based finetuning in Section 3.4 and it uses Eq. (1) as the training loss.

Table 7: Testing Accuracy of VLLaVO (w/o PseudoLabels) for UDA tasks on the *DomainNet* dataset.

	C	I	P	Q	R	S	Avg
C	-	54.9	70.7	19.9	86.5	73.9	61.2
I	81.5	-	72.2	21.3	86.6	72.9	66.9
P	81.4	54.5	-	17.5	86.3	72.2	62.4
Q	77.2	49.6	64.5	-	82.9	69.3	68.7
R	82.8	55.0	72.6	18.6	-	73.2	60.4
S	82.2	54.2	74.5	21.4	86.3	-	63.7
Avg	81.0	53.6	70.9	19.7	85.7	72.3	63.9

As shown in Table 7, VLLaVO (w/o PseudoLabels) is worse than VLLaVO (Table 3), showing that finetuning with pseudo-labels can boost the performance of VLLaVO. We further investigate the impact of the number of finetuning times on performance. Specifically, for each time of finetuning, we utilize the pseudo-label generated by the previous finetuned LLM. As shown in Table 13 of Appendix A.3, increasing the number of finetuning boosts the performance and will converge to the maximum. Considering the efficiency, our default VLLaVO entails a single pseudo-labeling-based finetuning for UDA.

4.4 Analysis

In this section, we aim to answer the following questions: (1) How can VLLaVO alleviate domain shifts? (2) How about the zero-shot capability of VLLaVO? (3) What information does the LLM within VLLaVO focus on?

VLLaVO is a Good Domain-Invariant Feature Learner. Figure 1 shows the t-SNE visualization [66] of feature embeddings of samples extracted from two domains (*i.e.*, Art painting and Cartoon) on the *PACS* dataset, where CLIP embeddings are extracted from the penultimate layer of the pre-trained CLIP image encoder, while LLM embeddings are obtained by averaging the last hidden state of the pre-trained LLaMA with $\mathbb{T}(\mathbf{x})$ as the input. As can be seen, in the visual modality shown in Figure 1a, samples from the same category have a noticeable domain shift, while, in the textual modality as shown in Figure 1b, samples from the same category are very close across the two domains, showing that the LLM can alleviate domain shifts. This observation gains additional support from Figure 4 in Appendix A.3, which presents the t-SNE visualization of Art and Real World domains on the *OfficeHome* dataset.

Moreover, Table 8 shows the frequency of domain-specific words per sample on the *PACS* dataset. As can be seen, the distribution of domain-specific words is different across domains, demonstrating that a domain gap exists in textual descriptions. Despite this domain gap, the finetuned LLMs exhibit strong performance, thereby confirming the effective handling of the visual domain gap by LLMs. Those results explain why the proposed VLLaVO uses LLMs to handle domain shifts in cross-domain learning.

Table 8: Word frequency per sample on the *PACS* dataset

words	A	C	P	S
painting	6.72	0.03	0.03	0.01
cartoon	0.12	3.77	0.00	0.36
camera	0.12	0.12	0.57	0.06
drawing	0.56	0.28	0.02	4.22

VLLaVO is a Good Zero-Shot Learner. To study the zero-shot ability of VLLaVO, we evaluate the cross-dataset performance of VLLaVO and zero-shot LLM (ZS-LLM) on DG datasets. Specifically, we select a DG dataset with the minimum number of samples (*i.e.*, *PACS*) as the source dataset, while considering the remaining DG datasets as the target datasets. All domains in the source dataset are merged for finetuning, and all domains in each target dataset are

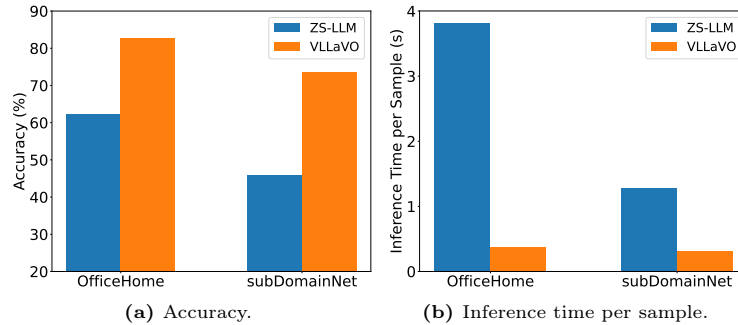


Fig. 3: Comparison between ZS-LLM and VLLaVO (finetuned on the *PACS* dataset). merged as well for testing. In this case, the cross-dataset setting is to test the zero-shot learning ability. For ZS-LLM, we follow [28] and directly feed $\mathbb{T}(\mathbf{x})$ into LLMs and compare the log-likelihood of each category. The category with the highest log-likelihood is chosen as the prediction. As mentioned in Section 4.1, the inference time of ZS-LLM is very costly for the *DomainNet* dataset with 345 categories. To reduce the computational demands associated with applying ZS-LLM to the *DomainNet* dataset, we create a subset of *DomainNet*, referred to as *subDomainNet*. This subset consists of the first 32 categories, arranged in alphabetical order.

Figure 3a shows the accuracy comparison between ZS-LLM and VLLaVO. As can be seen, the proposed VLLaVO outperforms ZS-LLM on the *OfficeHome* and *subDomainNet* datasets, verifying the superior zero-shot capability of VLLaVO. This can be attributed to the finetuning of VLLaVO on the designed question instruction template on *PACS*. This process significantly enhances the LLM understanding of the directives for the template \mathbb{T} . It enables more accurate predictions by deepening the comprehension of the relationships between $\mathbb{D}(\mathbf{x})$ and the category set.

To verify the efficiency of VLLaVO under the zero-shot condition, we compare the inference time per sample between VLLaVO and ZS-LLM. As shown in Figure 3b, compared with ZS-LLM, the inference of VLLaVO is consistent much faster on the *OfficeHome* and *subDomainNet* datasets.

What Information Does VLLaVO Focus On? To determine the crucial information that VLLaVO prioritizes, we use the gradient of the objective function with respect to each token embedding as a measure of sensitivity and importance, as discussed in [63, 80], to select important words within the descriptions. Specifically, for each word in the description, we calculate the mean absolute value of all the token gradients associated with that word as their sensitivity score. We then identify the Top-10 words with the highest scores by excluding the stop-words.

Example 2 shows an image of a house from the cartoon domain on the *PACS* dataset, and words marked by the red represent the Top-10 sensitive words that the LLM in VLLaVO primarily focuses on. As can be seen, the sensitive words

for the LLM can be categorized into two groups: (1) category words such as “house” and “bird” in the category set and (2) words related to the ground-truth label, *e.g.*, “schoolhouse”, “birdhouse”, “playhouse”, and “apartment”. Thus, after finetuning the LLM with the designed question instruction template, VLLaVO can focus on domain-invariant words that are related to classification tasks and disregard irrelevant words, further verifying the effectiveness of the proposed VLLaVO. More examples are shown in Appendix E.1.

Example 2: Textual Description $\mathbb{D}(x)$ of Image.

Tags:

- schoolhouse
- Property manager
- birdhouse
- Gingerbread house
- Playhouse

Attributes :

- house which is a building with walls and a roof
- residence which has windows
- property which has house, apartment, or other structure
- schoolhouse which typically large and rectangular in shape
- resident which has Background features such as furniture, buildings, other people

Captions:

- a picture of a house with a bird on the roof
- a cartoon house with a lot of windows
- a little house is outside a green bush
- a house with a bird sitting on top of it
- two story house with a roof with a brick chimney
- a cartoon house with a small window and red hat
- the cartoon house is next to a bird perched on a building
- a red roof and a yellow house with a bird
- a small brick building with a bird on top
- a house with a bird on the roof



(label: house)

5 Conclusion

In this paper, we propose VLLaVO to address visual domain shifts in visual cross-domain learning. VLLaVO uses VLMs for bridging the image and text modalities and finetunes the LLM using the designed question instruction template to focus on the domain-invariant features that are relevant to labels. VLLaVO excels in accurately identifying the correct category. The VLMs and LLM within VLLaVO could be substituted with any large-scale pretrained models. Extensive experiments demonstrate that VLLaVO achieves state-of-the-art performance in both DG and UDA benchmarks. To facilitate future research, we release a series of datasets in text modality for public use. In our future work, we will extend VLLaVO to other learning tasks.

References

1. Y. Zhang, S. Chen, W. Jiang, Y. Zhang, J. Lu, and J. T. Kwok, “Domain-guided conditional diffusion model for unsupervised domain adaptation,” *arXiv preprint arXiv:2309.14360*, 2023.
2. W. Jiang, Y. Zhang, and J. Kwok, “Effective structured prompting by meta-learning and representative verbalizer,” in *International Conference on Machine Learning*, 2023, pp. 15 186–15 199.
3. W. Jiang, H. Shi, L. Yu, Z. Liu, Y. Zhang, Z. Li, and J. T. Kwok, “Forward-backward reasoning in large language models for mathematical verification,” *arXiv preprint arXiv:2308.07758*, 2023.
4. L. Yu, W. Jiang, H. Shi, J. Yu, Z. Liu, Y. Zhang, J. T. Kwok, Z. Li, A. Weller, and W. Liu, “MetaMath: Bootstrap your own mathematical questions for large language models,” *arXiv preprint arXiv:2309.12284*, 2023.
5. C. Michaelis, B. Mitzkus, R. Geirhos, E. Rusak, O. Bringmann, A. S. Ecker, M. Bethge, and W. Brendel, “Benchmarking robustness in object detection: Autonomous driving when winter is coming,” *arXiv preprint arXiv:1907.07484*, 2019.
6. T. Sun, M. Segu, J. Postels, Y. Wang, L. Van Gool, B. Schiele, F. Tombari, and F. Yu, “Shift: a synthetic driving dataset for continuous multi-task domain adaptation,” in *Proceedings of the IEEE/CVF Conference on Computer Vision and Pattern Recognition*, 2022, pp. 21 371–21 382.
7. D. Dai and L. Van Gool, “Dark model adaptation: Semantic image segmentation from daytime to nighttime,” in *2018 21st International Conference on Intelligent Transportation Systems*. IEEE, 2018, pp. 3819–3824.
8. J. Cho, G. Nam, S. Kim, H. Yang, and S. Kwak, “Promptstyler: Prompt-driven style generation for source-free domain generalization,” in *Proceedings of the IEEE/CVF International Conference on Computer Vision*, 2023, pp. 15 702–15 712.
9. S. Menon and C. Vondrick, “Visual classification via description from large language models,” in *International Conference on Learning Representations*, 2023.
10. Z. Lai, N. Vesdapunt, N. Zhou, J. Wu, C. P. Huynh, X. Li, K. K. Fu, and C.-N. Chuah, “Padclip: Pseudo-labeling with adaptive debiasing in clip for unsupervised domain adaptation,” in *Proceedings of the IEEE/CVF International Conference on Computer Vision*, 2023, pp. 16 155–16 165.
11. V. Vapnik, *The nature of statistical learning theory*. Springer science & business media, 1999.
12. R. Xu, G. Li, J. Yang, and L. Lin, “Larger norm more transferable: An adaptive feature norm approach for unsupervised domain adaptation,” in *Proceedings of the IEEE/CVF International Conference on Computer Vision*, Oct. 2019.
13. Y. Ganin, E. Ustinova, H. Ajakan, P. Germain, H. Larochelle, F. Laviolette, M. Marchand, and V. Lempitsky, “Domain-adversarial training of neural networks,” *The Journal of Machine Learning Research*, vol. 17, no. 1, pp. 2096–2030, 2016.
14. M. Long, Z. Cao, J. Wang, and M. I. Jordan, “Conditional adversarial domain adaptation,” *Advances in Neural Information Processing Systems*, vol. 31, pp. 1640–1650, 2018.
15. H. Rangwani, S. K. Aithal, M. Mishra, A. Jain, and V. B. Radhakrishnan, “A closer look at smoothness in domain adversarial training,” in *International Conference on Learning Representations*, vol. 162. PMLR, 2022, pp. 18 378–18 399.

16. Y. Zhang, X. Wang, J. Liang, Z. Zhang, L. Wang, R. Jin, and T. Tan, “Free lunch for domain adversarial training: Environment label smoothing,” in *International Conference on Learning Representations*, 2023.
17. Y. Jin, X. Wang, M. Long, and J. Wang, “Minimum class confusion for versatile domain adaptation,” in *European Conference on Computer Vision*. Springer, 2020, pp. 464–480.
18. T. Xu, W. Chen, P. WANG, F. Wang, H. Li, and R. Jin, “CDTrans: Cross-domain transformer for unsupervised domain adaptation,” in *International Conference on Learning Representations*, 2022.
19. Y. Shu, X. Guo, J. Wu, X. Wang, J. Wang, and M. Long, “Clipood: Generalizing clip to out-of-distributions,” in *International Conference on Machine Learning*, 2023.
20. D. Li, Y. Yang, Y.-Z. Song, and T. M. Hospedales, “Deeper, broader and artier domain generalization,” in *Proceedings of the IEEE/CVF International Conference on Computer Vision*, 2017, pp. 5542–5550.
21. J. Cha, K. Lee, S. Park, and S. Chun, “Domain generalization by mutual-information regularization with pre-trained models,” in *European Conference on Computer Vision*. Springer, 2022, pp. 440–457.
22. J. Cha, S. Chun, K. Lee, H.-C. Cho, S. Park, Y. Lee, and S. Park, “Swad: Domain generalization by seeking flat minima,” *Advances in Neural Information Processing Systems*, vol. 34, pp. 22 405–22 418, 2021.
23. A. Radford, J. W. Kim, C. Hallacy, A. Ramesh, G. Goh, S. Agarwal, G. Sastry, A. Askell, P. Mishkin, J. Clark *et al.*, “Learning transferable visual models from natural language supervision,” in *International Conference on Machine Learning*. PMLR, 2021, pp. 8748–8763.
24. C. Fang, Y. Xu, and D. N. Rockmore, “Unbiased metric learning: On the utilization of multiple datasets and web images for softening bias,” in *Proceedings of the IEEE International Conference on Computer Vision*, 2013, pp. 1657–1664.
25. W. Berrios, G. Mittal, T. Thrush, D. Kiela, and A. Singh, “Towards language models that can see: Computer vision through the lens of natural language,” *arXiv preprint arXiv:2306.16410*, 2023.
26. J.-B. Alayrac, J. Donahue, P. Luc, A. Miech, I. Barr, Y. Hasson, K. Lenc, A. Mensch, K. Millican, M. Reynolds *et al.*, “Flamingo: a visual language model for few-shot learning,” *Advances in Neural Information Processing Systems*, vol. 35, pp. 23 716–23 736, 2022.
27. T. Brown, B. Mann, N. Ryder, M. Subbiah, J. D. Kaplan, P. Dhariwal, A. Neelakantan, P. Shyam, G. Sastry, A. Askell *et al.*, “Language models are few-shot learners,” *Advances in Neural Information Processing Systems*, vol. 33, pp. 1877–1901, 2020.
28. J. Wei, M. Bosma, V. Y. Zhao, K. Guu, A. W. Yu, B. Lester, N. Du, A. M. Dai, and Q. V. Le, “Finetuned language models are zero-shot learners,” *arXiv preprint arXiv:2109.01652*, 2021.
29. A. Fan, M. Lewis, and Y. Dauphin, “Hierarchical neural story generation,” in *Proceedings of the 56th Annual Meeting of the Association for Computational Linguistics*, 2018, pp. 889–898.
30. J. Li, D. Li, C. Xiong, and S. Hoi, “Blip: Bootstrapping language-image pre-training for unified vision-language understanding and generation,” in *International Conference on Machine Learning*. PMLR, 2022, pp. 12 888–12 900.
31. E. J. Hu, yelong shen, P. Wallis, Z. Allen-Zhu, Y. Li, S. Wang, L. Wang, and W. Chen, “LoRA: Low-rank adaptation of large language models,” in *International Conference on Learning Representations*, 2022.

32. X. Peng, B. Usman, N. Kaushik, J. Hoffman, D. Wang, and K. Saenko, “VisDA: The visual domain adaptation challenge,” Preprint arXiv:1710.06924, 2017.
33. K. Saenko, B. Kulis, M. Fritz, and T. Darrell, “Adapting visual category models to new domains,” in *Computer Vision—ECCV 2010: 11th European Conference on Computer Vision, Heraklion, Crete, Greece, September 5–11, 2010, Proceedings, Part IV 11*, vol. 6314. Springer, 2010, pp. 213–226.
34. K. Sohn, D. Berthelot, N. Carlini, Z. Zhang, H. Zhang, C. A. Raffel, E. D. Cubuk, A. Kurakin, and C.-L. Li, “Fixmatch: Simplifying semi-supervised learning with consistency and confidence,” *Advances in Neural Information Processing Systems*, vol. 33, pp. 596–608, 2020.
35. B. Zhang, Y. Wang, W. Hou, H. Wu, J. Wang, M. Okumura, and T. Shinozaki, “Flexmatch: Boosting semi-supervised learning with curriculum pseudo labeling,” *Advances in Neural Information Processing Systems*, vol. 34, pp. 18 408–18 419, 2021.
36. H. Venkateswara, J. Eusebio, S. Chakraborty, and S. Panchanathan, “Deep hashing network for unsupervised domain adaptation,” in *Proceedings of the IEEE/CVF Conference on Computer Vision and Pattern Recognition*, 2017, pp. 5018–5027.
37. O. Russakovsky, J. Deng, H. Su, J. Krause, S. Satheesh, S. Ma, Z. Huang, A. Karpathy, A. Khosla, M. Bernstein *et al.*, “Imagenet large scale visual recognition challenge,” *International Journal of Computer Vision*, vol. 115, pp. 211–252, 2015.
38. F.-F. Li and M. Andreeto, “Marc’aurelio ranzato, and pietro perona,” *Caltech*, vol. 101, p. 13, 2022.
39. M. Cimpoi, S. Maji, I. Kokkinos, S. Mohamed, and A. Vedaldi, “Describing textures in the wild,” in *Proceedings of the IEEE Conference on Computer Vision and Pattern Recognition*, 2014, pp. 3606–3613.
40. O. M. Parkhi, A. Vedaldi, A. Zisserman, and C. Jawahar, “Cats and dogs,” in *Proceedings of the IEEE/CVF Conference on Computer Vision and Pattern Recognition*. IEEE, 2012, pp. 3498–3505.
41. M.-E. Nilsback and A. Zisserman, “Automated flower classification over a large number of classes,” in *Indian Conference on Computer Vision, Graphics & Image Processing*. IEEE, 2008, pp. 722–729.
42. L. Bossard, M. Guillaumin, and L. Van Gool, “Food-101—mining discriminative components with random forests,” in *European Conference on Computer Vision*. Springer, 2014, pp. 446–461.
43. J. Xiao, J. Hays, K. A. Ehinger, A. Oliva, and A. Torralba, “Sun database: Large-scale scene recognition from abbey to zoo,” in *2010 IEEE Computer Society Conference on Computer Vision and Pattern Recognition*. IEEE, 2010, pp. 3485–3492.
44. J. Krause, M. Stark, J. Deng, and L. Fei-Fei, “3d object representations for fine-grained categorization,” in *Proceedings of the IEEE International Conference on Computer Vision Workshops*, 2013, pp. 554–561.
45. A. Gupta, P. Dollar, and R. Girshick, “Lvis: A dataset for large vocabulary instance segmentation,” in *Proceedings of the IEEE/CVF Conference on Computer Vision and Pattern Recognition*, 2019, pp. 5356–5364.
46. T.-Y. Lin, M. Maire, S. Belongie, J. Hays, P. Perona, D. Ramanan, P. Dollár, and C. L. Zitnick, “Microsoft coco: Common objects in context,” in *Computer Vision—ECCV 2014: 13th European Conference, Zurich, Switzerland, September 6–12, 2014, Proceedings, Part V 13*. Springer, 2014, pp. 740–755.

47. A. Kuznetsova, H. Rom, N. Alldrin, J. Uijlings, I. Krasin, J. Pont-Tuset, S. Kamali, S. Popov, M. Mallocci, A. Kolesnikov *et al.*, “The open images dataset v4: Unified image classification, object detection, and visual relationship detection at scale,” *International Journal of Computer Vision*, vol. 128, no. 7, pp. 1956–1981, 2020.
48. R. Krishna, Y. Zhu, O. Groth, J. Johnson, K. Hata, J. Kravitz, S. Chen, Y. Kalantidis, L.-J. Li, D. A. Shamma *et al.*, “Visual genome: Connecting language and vision using crowdsourced dense image annotations,” *International Journal of Computer Vision*, vol. 123, pp. 32–73, 2017.
49. P. Wang, Z. Zhang, Z. Lei, and L. Zhang, “Sharpness-aware gradient matching for domain generalization,” in *Proceedings of the IEEE/CVF Conference on Computer Vision and Pattern Recognition*, 2023, pp. 3769–3778.
50. M. Zhang, J. Yuan, Y. He, W. Li, Z. Chen, and K. Kuang, “Map: Towards balanced generalization of iid and ood through model-agnostic adapters,” in *Proceedings of the IEEE/CVF International Conference on Computer Vision*, 2023, pp. 11 921–11 931.
51. S. Rahman, P. Koniusz, L. Wang, L. Zhou, P. Moghadam, and C. Sun, “Learning partial correlation based deep visual representation for image classification,” in *Proceedings of the IEEE/CVF Conference on Computer Vision and Pattern Recognition*, 2023, pp. 6231–6240.
52. Z. Lin, Y. Wang, J. Zhang, and X. Chu, “Dynamicdet: A unified dynamic architecture for object detection,” in *Proceedings of the IEEE/CVF Conference on Computer Vision and Pattern Recognition*, 2023, pp. 6282–6291.
53. Z. Wan, Y. Zhang, Y. Wang, F. Cheng, and S. Kurohashi, “Reformulating domain adaptation of large language models as adapt-retrieve-revise,” *arXiv preprint arXiv:2310.03328*, 2023.
54. S. Shahtalebi, J.-C. Gagnon-Audet, T. Laleh, M. Faramarzi, K. Ahuja, and I. Rish, “Sand-mask: An enhanced gradient masking strategy for the discovery of invariances in domain generalization,” *arXiv preprint arXiv:2106.02266*, 2021.
55. C. Jia, Y. Yang, Y. Xia, Y.-T. Chen, Z. Parekh, H. Pham, Q. Le, Y.-H. Sung, Z. Li, and T. Duerig, “Scaling up visual and vision-language representation learning with noisy text supervision,” in *International Conference on Machine Learning*. PMLR, 2021, pp. 4904–4916.
56. P. Gao, S. Geng, R. Zhang, T. Ma, R. Fang, Y. Zhang, H. Li, and Y. Qiao, “Clip-adapter: Better vision-language models with feature adapters,” *International Journal of Computer Vision*, pp. 1–15, 2023.
57. Y. Lu, J. Liu, Y. Zhang, Y. Liu, and X. Tian, “Prompt distribution learning,” in *Proceedings of the IEEE/CVF Conference on Computer Vision and Pattern Recognition*, 2022, pp. 5206–5215.
58. K. Zhou, J. Yang, C. C. Loy, and Z. Liu, “Conditional prompt learning for vision-language models,” in *Proceedings of the IEEE/CVF Conference on Computer Vision and Pattern Recognition*, 2022, pp. 16 816–16 825.
59. Y. Wang, Z. Yu, J. Wang, Q. Heng, H. Chen, W. Ye, R. Xie, X. Xie, and S. Zhang, “Exploring vision-language models for imbalanced learning,” *International Journal of Computer Vision*, 2023.
60. C. Ge, R. Huang, M. Xie, Z. Lai, S. Song, S. Li, and G. Huang, “Domain adaptation via prompt learning,” *arXiv preprint arXiv:2202.06687*, 2022.
61. A. Yan, Y. Wang, Y. Zhong, C. Dong, Z. He, Y. Lu, W. Y. Wang, J. Shang, and J. McAuley, “Learning concise and descriptive attributes for visual recognition,” in *Proceedings of the IEEE/CVF International Conference on Computer Vision*, 2023, pp. 3090–3100.

62. W. Wang, Z. Chen, X. Chen, J. Wu, X. Zhu, G. Zeng, P. Luo, T. Lu, J. Zhou, Y. Qiao *et al.*, “Visionllm: Large language model is also an open-ended decoder for vision-centric tasks,” *arXiv preprint arXiv:2305.11175*, 2023.
63. H. He, J. Cai, J. Zhang, D. Tao, and B. Zhuang, “Sensitivity-aware visual parameter-efficient fine-tuning,” in *Proceedings of the IEEE/CVF International Conference on Computer Vision*, 2023, pp. 11 825–11 835.
64. X. Zhang, S. S. Gu, Y. Matsuo, and Y. Iwasawa, “Domain prompt learning for efficiently adapting clip to unseen domains,” *arXiv e-prints*, pp. arXiv–2111, 2021.
65. —, “Domain prompt learning for efficiently adapting clip to unseen domains,” *Transactions of the Japanese Society for Artificial Intelligence*, vol. 38, no. 6, pp. B–MC2_1, 2023.
66. L. Van der Maaten and G. Hinton, “Visualizing data using t-SNE,” *Journal of Machine Learning Research*, vol. 9, no. 11, pp. 2579–2625, Nov. 2008.
67. K. He, X. Zhang, S. Ren, and J. Sun, “Deep residual learning for image recognition,” in *Proceedings of the IEEE Conference on Computer Vision and Pattern Recognition*, 2016, pp. 770–778.
68. H. Touvron, M. Cord, M. Douze, F. Massa, A. Sablayrolles, and H. Jégou, “Training data-efficient image transformers & distillation through attention,” in *International Conference on Machine Learning*. PMLR, 2021, pp. 10 347–10 357.
69. Y. Zhang, Y. Li, L. Cui, D. Cai, L. Liu, T. Fu, X. Huang, E. Zhao, Y. Zhang, Y. Chen *et al.*, “Siren’s song in the ai ocean: A survey on hallucination in large language models,” *arXiv preprint arXiv:2309.01219*, 2023.
70. F. Shi, X. Chen, K. Misra, N. Scales, D. Dohan, E. H. Chi, N. Schärli, and D. Zhou, “Large language models can be easily distracted by irrelevant context,” in *International Conference on Machine Learning*. PMLR, 2023, pp. 31 210–31 227.
71. I. Gulrajani and D. Lopez-Paz, “In search of lost domain generalization,” in *International Conference on Learning Representations*, 2021.
72. H. Touvron, L. Martin, K. Stone, P. Albert, A. Almahairi, Y. Babaei, N. Bashlykov, S. Batra, P. Bhargava, S. Bhosale *et al.*, “Llama 2: Open foundation and fine-tuned chat models,” *arXiv preprint arXiv:2307.09288*, 2023.
73. I. Sutskever, O. Vinyals, and Q. V. Le, “Sequence to sequence learning with neural networks,” *Advances in Neural Information Processing Systems*, vol. 27, 2014.
74. A. Dosovitskiy, L. Beyer, A. Kolesnikov, D. Weissenborn, X. Zhai, T. Unterthiner, M. Dehghani, M. Minderer, G. Heigold, S. Gelly *et al.*, “An image is worth 16x16 words: Transformers for image recognition at scale,” in *International Conference on Learning Representations*, Oct. 2020, pp. 1–12.
75. I. Loshchilov and F. Hutter, “Decoupled weight decay regularization,” in *International Conference on Learning Representations*, 2019.
76. C. Raffel, N. Shazeer, A. Roberts, K. Lee, S. Narang, M. Matena, Y. Zhou, W. Li, and P. J. Liu, “Exploring the limits of transfer learning with a unified text-to-text transformer,” *The Journal of Machine Learning Research*, vol. 21, no. 1, pp. 5485–5551, 2020.
77. Z. Zhang, A. Zhang, M. Li, H. Zhao, G. Karypis, and A. Smola, “Multimodal chain-of-thought reasoning in language models,” *arXiv preprint arXiv:2302.00923*, 2023.
78. J. Wei, X. Wang, D. Schuurmans, M. Bosma, F. Xia, E. Chi, Q. V. Le, D. Zhou *et al.*, “Chain-of-thought prompting elicits reasoning in large language models,” *Advances in Neural Information Processing Systems*, vol. 35, pp. 24 824–24 837, 2022.

79. W. X. Zhao, K. Zhou, Z. Gong, B. Zhang, Y. Zhou, J. Sha, Z. Chen, S. Wang, C. Liu, and J.-R. Wen, “Jiuzhang: A chinese pre-trained language model for mathematical problem understanding,” in *Proceedings of the 28th ACM SIGKDD Conference on Knowledge Discovery and Data Mining*, 2022, pp. 4571–4581.
80. S. Feng, E. Wallace, A. Grissom II, M. Iyyer, P. Rodriguez, and J. Boyd-Graber, “Pathologies of neural models make interpretations difficult,” in *Proceedings of the 2018 Conference on Empirical Methods in Natural Language Processing*, 2018, pp. 3719–3728.
81. H. Xia and Z. Ding, “Structure preserving generative cross-domain learning,” in *Proceedings of the IEEE/CVF Conference on Computer Vision and Pattern Recognition*, 2020, pp. 4364–4373.
82. P. Zhang, H. Dou, Y. Yu, and X. Li, “Adaptive cross-domain learning for generalizable person re-identification,” in *European Conference on Computer Vision*. Springer, 2022, pp. 215–232.
83. K. Zhou, Z. Liu, Y. Qiao, T. Xiang, and C. C. Loy, “Domain generalization: A survey,” *IEEE Transactions on Pattern Analysis and Machine Intelligence*, 2022.
84. A. Dubey, V. Ramanathan, A. Pentland, and D. Mahajan, “Adaptive methods for real-world domain generalization,” in *Proceedings of the IEEE/CVF Conference on Computer Vision and Pattern Recognition*, 2021, pp. 14 340–14 349.
85. H. W. Chung, L. Hou, S. Longpre, B. Zoph, Y. Tay, W. Fedus, Y. Li, X. Wang, M. Dehghani, S. Brahma *et al.*, “Scaling instruction-finetuned language models,” *arXiv preprint arXiv:2210.11416*, 2022.
86. H. Liu, C. Li, Q. Wu, and Y. J. Lee, “Visual instruction tuning,” in *Thirty-seventh Conference on Neural Information Processing Systems*, 2023.
87. L. Ouyang, J. Wu, X. Jiang, D. Almeida, C. Wainwright, P. Mishkin, C. Zhang, S. Agarwal, K. Slama, A. Ray *et al.*, “Training language models to follow instructions with human feedback,” *Advances in Neural Information Processing Systems*, vol. 35, pp. 27 730–27 744, 2022.
88. Y. Wang, Y. Kordi, S. Mishra, A. Liu, N. A. Smith, D. Khashabi, and H. Hajishirzi, “Self-instruct: Aligning language model with self generated instructions,” *arXiv preprint arXiv:2212.10560*, 2022.
89. I. Radosavovic, R. P. Kosaraju, R. Girshick, K. He, and P. Dollár, “Designing network design spaces,” in *Proceedings of the IEEE/CVF Conference on Computer Vision and Pattern Recognition*, 2020, pp. 10 428–10 436.
90. M. Wortsman, G. Ilharco, J. W. Kim, M. Li, S. Kornblith, R. Roelofs, R. G. Lopes, H. Hajishirzi, A. Farhadi, H. Namkoong *et al.*, “Robust fine-tuning of zero-shot models,” in *Proceedings of the IEEE/CVF Conference on Computer Vision and Pattern Recognition*, 2022, pp. 7959–7971.
91. J. Zhu, H. Bai, and L. Wang, “Patch-mix transformer for unsupervised domain adaptation: A game perspective,” in *Proceedings of the IEEE/CVF Conference on Computer Vision and Pattern Recognition*, 2023, pp. 3561–3571.
92. Z. Liu, Y. Lin, Y. Cao, H. Hu, Y. Wei, Z. Zhang, S. Lin, and B. Guo, “Swin transformer: Hierarchical vision transformer using shifted windows,” in *Proceedings of the IEEE/CVF International Conference on Computer Vision*, 2021, pp. 10 012–10 022.
93. Z. Chai and C. Zhao, “Fault-prototypical adapted network for cross-domain industrial intelligent diagnosis,” *IEEE Transactions on Automation Science and Engineering*, vol. 19, no. 4, pp. 3649–3658, 2021.
94. N. Houlsby, A. Giurgiu, S. Jastrzebski, B. Morrone, Q. De Laroussilhe, A. Gesmundo, M. Attariyan, and S. Gelly, “Parameter-efficient transfer learning for nlp,” in *International Conference on Machine Learning*. PMLR, 2019, pp. 2790–2799.

95. O. Yoran, T. Wolfson, O. Ram, and J. Berant, “Making retrieval-augmented language models robust to irrelevant context,” *arXiv preprint arXiv:2310.01558*, 2023.
96. A. Creswell, M. Shanahan, and I. Higgins, “Selection-inference: Exploiting large language models for interpretable logical reasoning,” in *International Conference on Learning Representations*, 2023.
97. W. Sun, Z. Shi, S. Gao, P. Ren, M. de Rijke, and Z. Ren, “Contrastive learning reduces hallucination in conversations,” in *Proceedings of the AAAI Conference on Artificial Intelligence*, vol. 37, no. 11, 2023, pp. 13 618–13 626.
98. R. Zhong, K. Lee, Z. Zhang, and D. Klein, “Adapting language models for zero-shot learning by meta-tuning on dataset and prompt collections,” *arXiv preprint arXiv:2104.04670*, 2021.
99. Q. Yang, Y. Zhang, W. Dai, and S. J. Pan, *Transfer learning*. Cambridge, U.K.: Cambridge Univ. Press, 2020.
100. K. Zhou, J. Yang, C. C. Loy, and Z. Liu, “Learning to prompt for vision-language models,” *International Journal of Computer Vision*, vol. 130, no. 9, pp. 2337–2348, 2022.
101. T. Chen, S. Kornblith, M. Norouzi, and G. Hinton, “A simple framework for contrastive learning of visual representations,” in *International Conference on Machine Learning*. PMLR, 2020, pp. 1597–1607.
102. P. Foret, A. Kleiner, H. Mobahi, and B. Neyshabur, “Sharpness-aware minimization for efficiently improving generalization,” in *International Conference on Learning Representations*, 2020.
103. Y. Li, X. Tian, M. Gong, Y. Liu, T. Liu, K. Zhang, and D. Tao, “Deep domain generalization via conditional invariant adversarial networks,” in *Proceedings of the European Conference on Computer Vision*, 2018, pp. 624–639.
104. M. Long, Y. Cao, J. Wang, and M. Jordan, “Learning transferable features with deep adaptation networks,” in *International Conference on Machine Learning*. PMLR, 2015, pp. 97–105.
105. K. Zhou, Y. Yang, Y. Qiao, and T. Xiang, “Domain generalization with mixstyle,” *arXiv preprint arXiv:2104.02008*, 2021.
106. J. Wang, Z. Yang, X. Hu, L. Li, K. Lin, Z. Gan, Z. Liu, C. Liu, and L. Wang, “Git: A generative image-to-text transformer for vision and language,” *Transactions on Machine Learning Research*, 2022.
107. X. Wang, P. Guo, and Y. Zhang, “Unsupervised domain adaptation via bidirectional cross-attention transformer,” in *Joint European Conference on Machine Learning and Knowledge Discovery in Databases*. Springer, 2023, pp. 309–325.

Appendix

A Experiment

A.1 Datasets.

Tables 9 and 10 summarize the number of images, classes, domains, and tasks of datasets under the DG and UDA settings, respectively. Taking the *PACS* dataset as an example, the set of categories is “dog, elephant, giraffe, guitar, horse, house, person”.

Table 9: Statistics of the DG datasets used.

Dataset	#images	#classes	#domains	#tasks
<i>PACS</i>	9,991	7	4	4
<i>OfficeHome</i>	15,500	65	4	4
<i>DomainNet</i>	586,575	345	6	6

Table 10: Statistics of the UDA datasets used.

Dataset	#images	#classes	#domains	#tasks
<i>OfficeHome</i>	15,500	65	4	12
<i>DomainNet</i>	586,575	345	6	30

A.2 Implementation Details.

For the DG experiments, we utilize the CLIP-ViT-H-14 model⁴ as the default CLIP model for extracting tags and attributes. For generating captions, we employ the BLIP-large captioning checkpoint⁵. The values of K , M , and N used in the image-to-text extraction are all set to 5. We adopt LLaMA-2-7B [72] as the base LLM, and train it by LoRA finetuning [31] with rank 8 and α as 16. We use a batch size of 128 and the AdamW optimizer [75] with a learning rate of 0.001, $\beta_1 = 0.9$, $\beta_2 = 0.999$, and $\epsilon = 10^{-8}$. The LLM is finetuned for 100 steps on all datasets except the largest *DomainNet* dataset which uses 200 steps. To generate answers, we employ beam search [73] with a beam width of 4.

For the UDA experiments, we finetune LLM and finetune LLM with pseudo-labels for both 2 epochs. The other training settings are consistent with the above DG.

A.3 More Experimental Results.

Table 11 shows the testing accuracies of VLLaVO with variants of the textual description for UDA tasks on the *OfficeHome* dataset. As can be seen, VLLaVO with tags, attributes, and captions achieves the best performance.

⁴ <https://huggingface.co/laion/CLIP-ViT-H-14-laion2B-s32B-b79K>

⁵ <https://huggingface.co/Salesforce/blip-image-captioning-large>

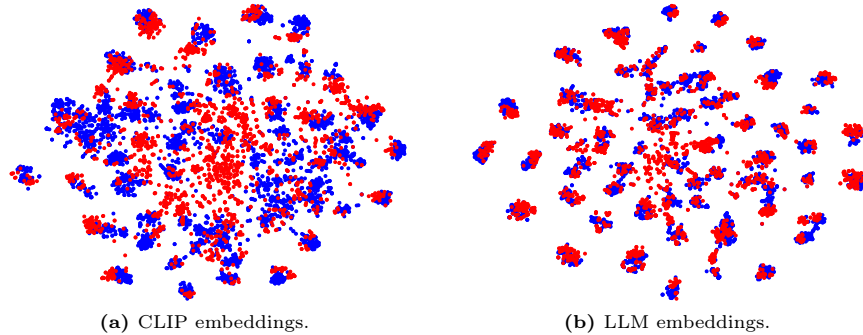


Fig. 4: t-SNE visualization of samples from the Real World domain (marked in red color) and the Art domain (marked in blue color) on the *OfficeHome* dataset.

Table 12 shows the testing accuracies of different LLMs for UDA tasks on the *OfficeHome* dataset. As can be seen, VLLaVO (w/ LLaMA2-7B) achieves the best performance, and VLLaVO (w/ FLAN-T5-base) still outperforms the previous SOTA method.

Figure 4 shows the t-SNE visualization of feature embeddings of samples extracted from two domains (*i.e.*, Art and Real World) on the *OfficeHome* dataset, where CLIP embeddings are extracted from the penultimate layer of pretrained CLIP image encoder, while LLM embeddings are obtained by averaging the last hidden state of pretrained LLaMA with $\mathbb{T}(x)$ as the input. As can be seen, the domain shift in LLM embeddings is smaller than that of CLIP embeddings, indicating the effectiveness of using LLM embeddings in cross-domain learning.

Table 11: Effects of different textual descriptions for UDA tasks on the *OfficeHome* dataset. The best is in **bold**.

Tags	Attributes	Captions	A→C	A→P	A→R	C→A	C→P	C→R	P→A	P→C	P→R	R→A	R→C	R→P	Avg
✓	✗	✗	77.3	90.3	89.2	83.7	94.0	91.6	82.3	78.8	90.4	83.1	79.5	94.3	86.2
✗	✓	✗	76.5	94.0	89.7	79.2	95.4	91.5	78.0	78.4	90.5	78.8	78.2	95.2	85.4
✗	✗	✓	85.1	95.5	91.3	87.8	94.9	91.7	84.8	83.2	90.9	87.8	82.8	95.2	89.3
✓	✓	✓	85.4	96.6	94.1	90.3	97.1	94.4	87.9	85.7	94.5	90.1	85.5	97.3	91.6

Table 12: Effects of different LLMs for UDA tasks on the *OfficeHome* dataset. The best is in **bold**.

Method	A→C	A→P	A→R	C→A	C→P	C→R	P→A	P→C	P→R	R→A	R→C	R→P	Avg
Previous SOTA [10]	76.4	90.6	90.8	86.7	92.3	92.0	86.0	74.5	91.5	86.9	79.1	93.1	86.7
VLLaVO (w/ FLAN-T5-base)	82.0	94.4	89.7	86.1	92.6	90.4	85.6	83.9	88.5	88.8	84.5	93.3	88.3
VLLaVO (w/ LLaMA2-7B)	85.4	96.6	94.1	90.3	97.1	94.4	87.3	85.7	94.5	90.1	85.5	97.3	91.5

In VLLaVO, we only finetune with pseudo-labels for only one time. Obviously, we can do that for multiple times. To identify the effect of the times of finetuning with pseudo-labels on the performance, Table 13 shows the testing

Table 13: Effects of the time of finetuning with pseudo-label for UDA tasks on the *OfficeHome* dataset. The best is in **bold**.

#Finetuning	A→C	A→P	A→R	C→A	C→P	C→R	P→A	P→C	P→R	R→A	R→C	R→P	Avg
0	85.0	96.2	93.9	89.4	96.8	94.1	87.5	85.4	94.5	90.2	85.3	97.1	91.3
1 (default)	85.4	96.6	94.1	90.3	97.1	94.4	87.9	85.7	94.5	90.1	85.5	97.3	91.6
2	85.6	96.8	94.3	90.4	97.1	94.7	88.2	85.8	94.4	89.9	85.5	97.5	91.7
3	85.5	96.9	94.5	90.5	97.2	94.9	88.4	85.7	94.5	90.0	85.6	97.5	91.8
4	85.5	97.0	94.6	90.2	97.3	95.0	88.2	85.7	94.4	90.3	85.8	97.5	91.8
5	85.4	97.0	94.8	90.6	97.4	94.9	88.3	85.6	94.5	90.4	85.8	97.5	91.8

accuracies with different times of finetuning with pseudo-labels for UDA tasks on the *OfficeHome* dataset. According to the results, we can see that when the time increases from 0 to 3, the performance becomes better in terms of the average performance, and after that, the average performance becomes stable. Those results demonstrate the effectiveness of finetuning with pseudo-labels. However, with increasing times of finetuning with pseudo-labels, the time cost increases. So by default, we conduct only one finetuning with pseudo-labels.

A.4 Effect of Instruction Template

To verify the effectiveness of the designed question instruction template, we compare VLLaVO with its variants: VLLaVO (w/ domain information) and VLLaVO (w/ simple template). For VLLaVO (w/ domain information), we further consider the domain information in DG. Specifically, we add the domain name of each sample, denoted as $\{\text{Domain Name}\}$, to the designed question instruction. With the domain name, the template $\mathbb{T}(\mathbf{x})$ is shown in Example 3. For VLLaVO (w/ simple template), we use the template $\hat{\mathbb{T}}(\mathbf{x})$ shown in Example 4, which only employs the $\{\mathbb{D}(\mathbf{x})\}$ to formulate the question instruction.

Example 3: Template $\mathbb{T}(\mathbf{x})$.

Give the information about a $\{\text{Domain Name}\}$ image: $\{\mathbb{D}(\mathbf{x})\}$.
 According to the information, choose the most similar category from the given options: $\{\text{Category Set}\}$.
 ### Answer:

Example 4: Template $\hat{\mathbb{T}}(\mathbf{x})$.

$\{\mathbb{D}(\mathbf{x})\}$.
 ### Answer:

Table 14 shows the testing accuracies of DG tasks on the *OfficeHome* dataset by using the setting in Section 4.1. As can be seen, similar cross-domain performance is achieved with or without the domain information. Therefore, for simplicity, we do not consider the domain information in VLLaVO. Moreover, VLLaVO outperforms VLLaVO (w/ simple template), showing the rationality of our designed template.

Table 14: Effects of instruction templates for DG tasks on the *OfficeHome* dataset. The best is in **bold**.

Method	A	C	P	R	Avg
VLLaVO	90.0	86.7	97.4	95.1	92.3
VLLaVO (w/ domain information)	90.4	86.5	97.3	95.2	92.4
VLLaVO (w/ simple template)	89.4	85.8	97.0	94.9	91.8

B Released Text Datasets

Table 15: Statistics of the released text datasets.

Dataset	#samples	#classes	#domains
<i>PACS</i>	9,991	7	4
<i>OfficeHome</i>	15,500	65	4
<i>DomainNet</i>	586,575	345	6

We release three datasets⁶ constructed from cross-domain image datasets, including *PACS*, *OfficeHome*, and *DomainNet*. Each dataset contains multiple domains as in the corresponding image dataset. Each sample in a domain of one dataset contains the textual description, which is constructed in Section 3.2, for the corresponding image and the label is just the label of the corresponding image. Hence, each dataset released is for multi-domain text classification tasks. These datasets collectively contain 612,066 samples in total. Table 15 summarizes the statistics of those datasets, including the number of samples, classes, and domains.

C Algorithms

The training pipeline of VLLaVO is summarized in Algorithm 1. To begin with, VLLaVO generates textual descriptions of images using pre-trained VLMs. After obtaining textual descriptions, we finetune an LLM with the designed question instruction template that combines the textual descriptions and their category labels. Moreover, when employing VLLaVO for UDA, the LLM is finetuned in the source domain to generate the pseudo-labels for target domain samples. The LLM is then finetuned with both target domain samples with pseudo-labels and source domain samples with ground truth labels.

D Limitation

Despite showing promising results in various cross-domain tasks, the VLLaVO has certain limitations. Firstly, the quality of the extracted textual descriptions relies on the capabilities of the VLMs and there is still room for further improvement. Examples of these textual descriptions can be found in Section E.1. While

⁶ They are available at <https://www.dropbox.com/scl/fo/brzj14xzpfzf0r57tkkwr/h?rlkey=zxeabnjpkgbpwugskpcjzrqa&dl=0>.

Algorithm 1 Training pipeline of VLLaVO

Input: Source domain \mathcal{D} , trainable LLM parameters θ , description template \mathbb{D} , instruction template \mathbb{T} , learning rate η .

- 1: Initialize θ ;
- 2: **if** Apply to UDA **then**
- 3: $\hat{\theta} = \theta$;
- 4: **end if**
- 5: **repeat**
- 6: Sample an image (\mathbf{x}, y) from \mathcal{D} ;
- 7: Extract $\mathbb{D}(\mathbf{x})$ using VLMS via Section 3.2;
- 8: Generate $\mathbb{T}(\mathbf{x})$ using $\mathbb{D}(\mathbf{x})$;
- 9: $\mathcal{L}_{dg}(\theta) = -\log p_{\theta}(y|\mathbb{T}(\mathbf{x}))$;
- 10: $\theta = \theta - \eta \nabla_{\theta} \mathcal{L}_{dg}(\theta)$;
- 11: **until** converged.
- 12: **if** Apply to UDA **then**
- 13: **repeat**
- 14: Sample an image \mathbf{x} from $\mathcal{D} \cup \mathcal{T}$;
- 15: Extract $\mathbb{D}(\mathbf{x})$ using VLMS via Section 3.2;
- 16: Generate $\mathbb{T}(\mathbf{x})$ using $\mathbb{D}(\mathbf{x})$;
- 17: **if** $\mathbf{x} \in \mathcal{T}$ **then**
- 18: $\hat{y} = LLM(\mathbb{T}(\mathbf{x}); \theta)$;
- 19: $\mathcal{L}(\theta) = -\log p_{\hat{\theta}}(\hat{y}|\mathbb{T}(\mathbf{x}))$;
- 20: $\hat{\theta} = \hat{\theta} - \eta \nabla_{\hat{\theta}} \mathcal{L}(\theta)$;
- 21: **else**
- 22: $\mathcal{L}(\theta) = -\log p_{\hat{\theta}}(y|\mathbb{T}(\mathbf{x}))$;
- 23: $\hat{\theta} = \hat{\theta} - \eta \nabla_{\hat{\theta}} \mathcal{L}(\theta)$;
- 24: **end if**
- 25: **until** converged.
- 26: $\theta = \hat{\theta}$;
- 27: **end if**
- 28: **return** θ

most descriptions align well with the images, there are a few instances where the descriptions do not accurately match the images. Secondly, our current work focuses solely on the visual classification task. However, the domain shifts may also exist in the other visual tasks (*e.g.*, segmentation, depth estimation, and surface normal prediction). Future research should explore methods to leverage the capabilities of LLMs in handling these types of visual cross-domain tasks.

E Case Study

E.1 More Examples of Textual Description

Example 5, 6, and 7 show textual descriptions for images of different categories on the *PACS* dataset, while Example 8 and 9 show textual descriptions for images of different categories on the *OfficeHome* dataset. The Top-10 sensitive word (excluding stop words) is highlighted in red.

Example 5: Textual Description $\mathbb{D}(x)$ of Image x .

Tags:

- giraffe
- Giraffidae
- Watercolor paint
- Camelid
- Animal product



(label: giraffe)

Attributes:

- giraffe which has dark spots on the coat
- giraffe which has long neck
- giraffe which has cloven hooves
- animal which has muzzle
- artwork which is a creative work of art, such as a painting, sculpture, drawing, or photograph

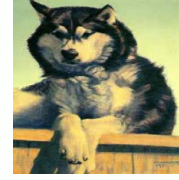
Captions:

- a giraffe with pink colored hair walking
- a closeup view of a giraffe with a very very painted look on his face
- a painting of a giraffe with its tongue hanging out
- the giraffe is wearing a crown and with his tongue out
- a watercolor painting of a giraffe with a tongue out
- a watercolor portrait of an adorable giraffes face
- a giraffe staring at the camera with a paint splatter effect
- a painting of a giraffe on a wall
- an artistic picture of a giraffe with a colorful head piece
- an image of a giraffe that is on a canvas

Example 6: Textual Description $\mathbb{D}(x)$ of Image x .

Tags:

- Sled **dog**
- Alaskan **malamute**
- Siberian **husky**
- Seppala siberian **sleddog**
- Sakhalin **husky**



(label: dog)

Attributes:

- alaskan **malamute** which has black, grey, white, or sable coat with a mask-like pattern on the **face**
- siberian **husky** which has dense undercoat with a longer, thicker outer coat
- alaskan **malamute** which has broad head
- alaskan **malamute** which has thick double coat of fur
- siberian **husky** which has thick double coat of fur

Captions:

- a painting of a **husky dog** with a **dog** bone on its paw
- a painting of a **dog** on a wooden deck
- an alaska wolf **dog** is **sitting** on a fence
- a black and white **husky dog sitting** in a bath tub
- a painting of a wolf laying on a ledge
- a **dog sitting** on top of a box next to a wall
- a cover of a book with a painting of a **husky dog**
- a **dog sitting** on a ledge looking into the distance
- a **dog** on top of a wooden wall with green sky in background
- a picture of a huge **dog sitting** down on the ledge

Example 7: Textual Description $\mathbb{D}(x)$ of Image x .

Tags:

- Mustang horse
- horse
- stallion
- forelock
- foal



(label: horse)

Attributes:

- horse which has mane of hair on neck
- stallion which has powerful build
- animal which has whiskers or mane -artwork which is a creative work of art, such as a painting, sculpture, drawing, or photograph
- horse which has furry body

Captions:

- a brown horse with its long mane running in the field
- a painting of a big brown horse with long mane
- a picture of a horse standing on a field
- an orange - colored horse walking across a green, yellow and yellow - green grassy area
- a painting of two horses in a field -the horse's head is shown with long hair hanging
- horses standing near each other in some grass
- a painting of a horse that is standing up by itself
- painting of a horse with a shaggy hair blowing in the wind
- a painting of a horse in a green field

Example 8: Textual Description $\mathbb{D}(x)$ of Image x .

Tags:

- saddlebag
- Road **bicycle**
- bicycle**
- Conference **Bike**
- Tandem **bicycle**



(label: bike)

Attributes:

- cyclist which is a saddle bag
- bike** which is a kickstand
- mountain **bike** which has kickstand
- mountain **bike** which has straight handlebars
- bike** which has handlebars

Captions:

- two backpacks and **bicycles** parked next to each other
- a **bicycle** with a bundle of luggage and **bags** parked at the side of a road
- a **bicycle** that is sitting in the grass
- a couple of bikes with **bags** strapped on a **bicycle** rack
- a **bike** has two wheels and has some **bags**
- a **bicycle** with a blue sack on the back and saddle attached
- a **bike** that is sitting next to the mountains
- a **bike**, loaded with a blue backpack, parked on a road
- a **bicycle** with two **bags** that include backpacks
- bicycle** with three **bags** on the back rack

Example 9: Textual Description $\mathbb{D}(x)$ of Image x .

Tags:

- Tin can
- pail
- Oyster pail
- Watering can
- cannister



(label: bucket)

Attributes:

- winebucket which has cylindrical or oval shape
- bucket which has cylindrical container
- pail which is a cylindrical or bucket
- shaped container
- pail which has usually has a lid
- pail which has usually has a handle

Captions:

- a green and rusty metal bucket sitting on a table
- a close up of a metal basket on a table
- a picture of a bucket filled with dirt
- an object with a holed handle on a small cup
- an empty green pot in a pink room
- a basket sitting in a room near a wall
- a large pot sitting on a counter
- a bucket that is green sitting on a table
- a green pot on a table on a pink background
- a rusted tin bucket sitting on a pink table

E.2 Examples of Undesirable Answers

To explore the reason behind the limited performance of ZS-LLM, in Table 16 we present a list of undesirable answers with the ‘person’ category on the *PACS* dataset. Specifically, we feed $\mathbb{T}(x)$ into the pretrained LLaMA and generate the corresponding output with beam search. As can be seen, undesirable answers can be categorized into two groups: (1) The answer is correlated to the label but represented in an undesirable way. It includes extraneous punctuation marks like “ ’ ” and “ [” as well as phrases such as “The most similar category to the given information” and reasons for classification. Those undesirable answers may be due to that the training objective in the next word prediction task during the pretraining process (*e.g.*, “The most similar”) is still misaligned with the expected zero-shot learning objective (*e.g.*, “person”). (2) Undesirable answers do not belong to the provided options. For instance, the answers in the last three rows mention “woman”, “man”, and “movie”. Those answers show that the pretrained language model is limited in its ability to follow instructions.

Table 16: Example of undesirable answers on the *PACS* dataset.

Label	Answer
person	'person'
person	['person']
person	The most similar category to the given information is 'person'.
person	The most similar category from the given options is 'person'.
person	The most similar category based on the information provided is ['person'].
person	The most similar category to the given information is 'person'. The image is of an astronaut in outer space, which is a subject or theme related to 'person'.
person	The most similar category to the given information is "person". The image is a painting of a person, specifically a man jumping over a crowd, standing over a bunch of people, or running with a group of others.
person	Given the information provided, the most similar category to the images is "person". This is because all of the images depict human figures, either as the main subject or as part of a larger scene. Therefore, the category "person".
person	The most similar category to the given information is 'woman'.
person	The most similar category to the given information is 'man'.
person	The most similar category to the given information is ['movie'].